Accumulation of Heavy Particles in Bounded Vortex Flows

Rutger H.A. IJzermans and R. Hagmeijer

University of Twente, P.O. Box 217, 7500 AE Enschede, The Netherlands;
e-mail: r.h.a.ijzermans@ctw.utwente.nl, r.hagmeijer@ctw.utwente.nl

Abstract. Much research has been done on the motion of heavy particles in simple vortex flows. In most of this work, particle motion is investigated under the influence of fixed vortices. In the context of astrophysics, the motion of heavy particles in rotating two-dimensional flows has been investigated; the rotation follows from the laws of Kepler. In the present paper, the motion of heavy particles in potential vortex flow in a circular domain is investigated. The vortex describes a circular trajectory due to the presence of the boundary, so that a steadily rotating flow is obtained. In order to isolate the effect of particle inertia, only Stokes drag is taken into account in the equation of motion. The numerical simulations are based on a one-way coupling. They show that small heavy particles accumulate in an ellitpic region of the flow, counterrotating with respect to the vortex. When the particle Stokes number exceeds a threshold, depending on the vortex configuration, particles are expelled from the circular domain. A stability criterion for this particle accumulation is derived analytically. These results are qualitatively comparable to those obtained by others in astrophysics.

1 Introduction

Gas-particle separators are used in some industrial processes. Their purpose is to separate liquid droplets or small heavy particles from gas flows. In general the separators consist of a cylindrical tube containing a region of high vorticity. In some applications this region of high vorticity has a helical shape. The goal of the present research is to determine the influence of this coherent structure of vorticity on the properties of heavy particle separation.

The configuration of a steady helical vortex filament in a cylindrical tube is sketched in Figure 1. The three-dimensional (potential) velocity field for this situation was first derived by Alekseenko et al. [1]. The calculation of this velocity field is far from trivial due to the torsion of the helical vortex filament.

If, however, the pitch of the helix is sufficiently large compared to the tube radius, the contribution due to the three-dimensionality of the helical vortex filament can be neglected. In this limit, the velocity field reduces to a superposition of a constant axial velocity and a time-dependent two-dimensional flow in the cross-sectional

S. Balachandar and A. Prosperetti (eds), Proceedings of the IUTAM Symposium on Computational Multiphase Flow, 75–85.

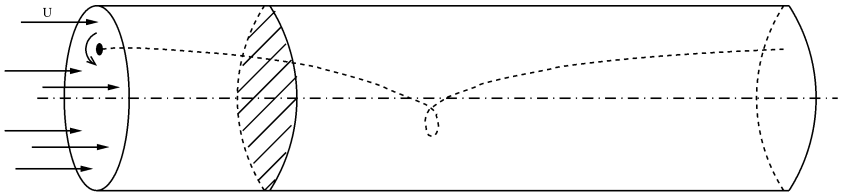

Fig. 1. Typical configuration of gas-liquid separator.

plane, moving with velocity U (see Figure 1). Here, we use this two-dimensional approximation. The two-dimensional flow is characterized by an eccentrically placed point vortex in a circular domain. The vortex rotates at constant angular velocity due to its self-induced motion.

The motion of heavy particles in dilute suspensions has received much attention in the past two decades. Investigations (e.g. [5–7]), have reported the motion of small heavy particles in elementary vortex flows. Most of them focussed on the motion of particles near fixed vortices. The general conclusion is that heavy particles are expelled from regions of high vorticity and tend to accumulate in regions of high strain. The particle segregation was shown to be highest for particles whose relaxation time corresponds to a typical time scale of the flow [4]. This causes also the effect of preferential concentration observed in turbulent flows [11].

The motion of heavy particles in two-dimensional rotating flows has been investigated in the context of planet formation from the solar nebula [3, 10]. The solar nebula is a collection of gas particles situated on a large disk, which rotates following the laws of Kepler. The turbulent flow in the solar nebula is approximately two-dimensional, so that large coherent vortex structures are likely to occur. Provenzale [10] gives a good overview of the motion of heavy particles in a two-dimensional flow field with a finite vorticity distribution. Chavanis [3] makes an analytical estimate of the time it takes to capture a heavy particle in an anticyclonic vortex, by assuming the flow to be a superposition of a prescribed elliptic patch of uniform vorticity and a steadily rotating Keplerian disk.

In this paper we investigate the motion of heavy particles in closed circular domains containing a point vortex. The presence of the boundary gives rise naturally to a steadily rotating flow field [9]. The focus in this paper will be on the accumulation of particles in certain flow regions due to their inertia. In order to isolate the effect of the particle inertia, the simulations are based on a one-way coupling. Gravity is neglected, since it is typically a minor effect in industrial gas-liquid separators. A stability criterion for particle accumulation is derived for any steadily rotating flow field which can be expressed in terms of a stream function. It is shown that the general results correspond to those obtained by Chavanis [3], Provenzale [10] and others.

The paper is organized as follows. In Section 2 we present the dynamical equations governing the motion of a point vortex on a unit disk. Besides, we give the equation of motion of passive tracers in such flow, and the equation of motion of heavy particles. In Section 3 we present the numerical results of motion of heavy

particles in a circular domain containing one vortex; analysis is used to explain the results for the trajectories of heavy particles in such flows. Finally, a summary and conclusions are given in Section 4.

2 Dynamical equations

The goal of the present research is to investigate the motion of heavy particles in a flow of one vortex on a disk. The governing equations are related to the motion of the point vortex under its self-induced velocity, to the motion of passive tracers in the flow and to the motion of small heavy particles in such flows. The equations governing these three types of motion are presented in this section.

2.1 Point vortex motion on a unit disk

Flows with N point vortices are singular solutions of the 2D Euler equations and can be seen as a Hamiltonian system. If the velocity field is divergence-free ($\nabla \cdot \boldsymbol{u} = 0$), the motion of passive tracers is governed by a stream function Ψ which plays the role of a Hamiltonian. It is well-known [9] that the motion of point vortices is Hamiltonian, too.

We consider the example of one point vortex on a disk. All variables are made dimensionless by the vortex strength and the cylinder radius. The distance from the vortex to the disk center is denoted by r_v. In order to satisfy the boundary condition (zero normal velocity on the circular boundary), a counter-rotating image vortex is placed outside the domain, on a distance $1/r_v$ ([9]).

The Hamiltonian, governing the motion of the vortex, becomes:

$$H = \frac{1}{4\pi} \ln\left[1 - x_v^2 - y_v^2\right], \tag{1}$$

so the motion of the vortex is:

$$\dot{x}_v = \frac{\partial H}{\partial y_v} = \frac{1}{2\pi}\left(\frac{-y_v}{1 - x_v^2 - y_v^2}\right), \qquad \dot{y}_v = -\frac{\partial H}{\partial x_v} = \frac{1}{2\pi}\left(\frac{x_v}{1 - x_v^2 - y_v^2}\right). \tag{2}$$

This shows that the vortex moves on a circle of constant radius $\sqrt{x_v^2 + y_v^2} = r_v$ with constant angular velocity. This angular velocity is here called $\dot{\theta}_v$ and is given by:

$$\dot{\theta}_v = \frac{1}{2\pi}\left(\frac{1}{1 - r_v^2}\right). \tag{3}$$

2.2 Passive tracers in bounded vortex flow

The time-dependent stream function governing the motion of passive tracers reads:

$$\Psi(x, y, t) = -\frac{1}{4\pi} \ln \frac{(x - x_v)^2 + (y - y_v)^2}{\left(x - (x_v/r_v^2)\right)^2 + \left(y - (y_v/r_v^2)\right)^2}. \tag{4}$$

Then, the velocity of passive tracers follows from:

$$U = \frac{\partial \Psi}{\partial y}, \qquad V = -\frac{\partial \Psi}{\partial x}. \tag{5}$$

The stream function can be simplified by applying the following coordinate transform:

$$\xi(x, y, t) \equiv x \cos\theta_v + y \sin\theta_v,$$
$$\eta(x, y, t) \equiv -x \sin\theta_v + y \cos\theta_v.$$

This means that a reference frame is chosen that rotates with the vortex. In this frame, we define:

$$\overline{\Psi}(\xi(x, y, t), \eta(x, y, t)) \equiv \Psi(\xi(x, y, t), \eta(x, y, t), 0) = \Psi(x, y, t). \tag{6}$$

Substituting the expression for $\overline{\Psi}$ and the coordinate transform into Equation (5) yields:

$$U = \sin\theta_v \frac{\partial \overline{\Psi}}{\partial \xi} + \cos\theta_v \frac{\partial \overline{\Psi}}{\partial \eta}, \tag{7}$$

$$V = -\cos\theta_v \frac{\partial \overline{\Psi}}{\partial \xi} + \sin\theta_v \frac{\partial \overline{\Psi}}{\partial \eta}. \tag{8}$$

Besides, it is easily derived that the velocity in the co-rotating frame, denoted by (υ, ν) satisfies:

$$\upsilon = U \cos\theta_v + V \sin\theta_v + \dot{\theta}_v \eta, \tag{9}$$
$$\nu = -U \sin\theta_v + V \cos\theta_v - \dot{\theta}_v \xi. \tag{10}$$

In order to obtain a stream function $\hat{\Psi}$ in the co-rotating frame such that:

$$\upsilon = \frac{\partial \hat{\Psi}}{\partial \eta}, \quad \nu = -\frac{\partial \hat{\Psi}}{\partial \xi}, \tag{11}$$

we define:

$$\hat{\Psi}(\xi, \eta) \equiv \overline{\Psi}(\xi, \eta) + \frac{1}{2}\dot{\theta}_v(\xi^2 + \eta^2). \tag{12}$$

The total stream function $\hat{\Psi}$ then reads:

$$\hat{\Psi}(\xi, \eta) = \frac{1}{2}\dot{\theta}_v\left(\xi^2 + \eta^2\right)^2 - \frac{1}{4\pi} \ln \frac{(\xi - r_v)^2 + \eta^2}{(r_v\xi - 1)^2 + r_v^2\eta^2}, \tag{13}$$

where, for convenience, the vortex is placed on the positive ξ-axis. Contour lines of the stream function are plotted in Figure 2 (see also [9], p. 135). The boundary of the circular domain is a streamline of the flow, as it should be in order to guarantee zero wall-normal velocity on the boundary.

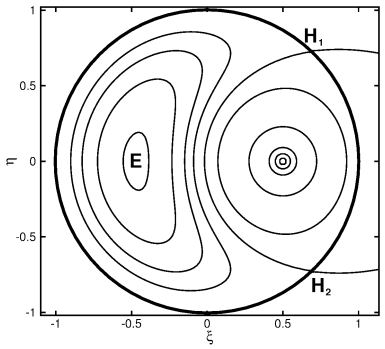

Fig. 2. Contour lines of stream function describing the motion of passive tracers in a one-vortex system, plotted in the frame rotating with the vortex; $r_v = 0.5$. H_1 and H_2 are hyperbolic stagnation points, E is an elliptic stagnation point.

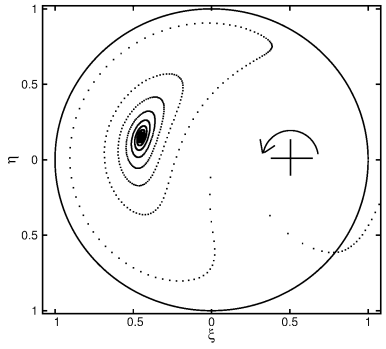

Fig. 3. Poincaré sections of 2 slipping particles in one-vortex system. $r_v = 0.5$; $St = 0.5$.

Stagnation points correspond to critical points of the stream function, i.e. points where the flow velocity is zero. The Hessian, which is defined as:

$$\mathcal{H} \equiv \hat{\Psi}_{\xi\xi}\hat{\Psi}_{\eta\eta} - \hat{\Psi}_{\xi\eta}^2, \tag{14}$$

is used to determine the character of the stagnation point (the subscripts indicate differentiation). With the Hessian in the stagnation point denoted by $\mathcal{H}_0$, the following classification can be made:

$$\begin{aligned} &\mathcal{H}_0 < 0 \Leftrightarrow \text{saddle point (hyperbolic point)},\\ &\mathcal{H}_0 > 0 \Leftrightarrow \text{extremum (elliptic point)}. \end{aligned} \tag{15}$$

With help of Equation (12), the Hessian can also be rewritten in terms of the stream function $\overline{\Psi}(\xi, \eta)$. Since $\nabla^2\overline{\Psi}(\xi, \eta) = 0$ (irrotational flow), it follows that:

$$\mathcal{H} = -\overline{\Psi}_{\xi\xi}^2 - \overline{\Psi}_{\xi\eta}^2 + \dot{\theta}_v^2. \tag{16}$$

From this it follows that if $\dot{\theta}_v = 0$, which corresponds to the instantaneous flow field in the quiescent frame, only hyperbolic stagnation points exist. If, on the other hand, $\dot{\theta}_v > 0$, then also an elliptic stagnation point may arise. This elliptic stagnation point is always counter-rotating (anticyclonic) with respect to $\dot{\theta}_v$.

An example of a rotating point vortex flow field with both hyperbolic and elliptic stagnation points is shown in Figure 2. This is the flow field induced by one single point vortex in a circular boundary, plotted in the frame rotating with the vortex. In this frame, the streamlines are independent of time.

2.3 Motion of heavy particles

Using the one-vortex flow as the background flow field, we now consider the motion of heavy particles in such a flow. The particles in relevant applications (such as small

iced droplets in gas-liquid separators) are small and to good approximation spherical. In most relevant applications of gas-liquid separators, the influence of gravity can be neglected. For the sake of simplicity, effects of inter-particle collisions are not taken into account. The particles are assumed not to influence the gas flow, so the approach presented here is based on a one-way coupling.

At the beginning of the simulation, the particles are assumed to have the same velocity as the local gas flow. The particles are allowed to cross the circular boundary, but this does not have a significant effect on the results: a particle that has left the domain does not enter it again.

The dynamical equations for small spherical particles have been established by Maxey and Riley [8]. Under the assumptions above they reduce to the following equation, which reads in a quiescent frame and in dimensionless form:

$$\frac{d\boldsymbol{x}_p}{dt} = \boldsymbol{u}_p, \tag{17}$$

$$\frac{d\boldsymbol{u}_p}{dt} = \frac{1}{St}(\boldsymbol{u}_g - \boldsymbol{u}_p). \tag{18}$$

where $\boldsymbol{x}_p$ and $\boldsymbol{u}_p$ are the position and the velocity of the particle respectively, $\boldsymbol{u}_g$ is the velocity of the gas. The parameter St is the Stokes number. This is the particle relaxation time made dimensionless with respect to the vortex strength and the cylinder radius:

$$St \equiv \frac{\tau_p \Gamma}{R^2}. \tag{19}$$

Particles with $St = 0$ will react instantaneously to changes in the flow and will thus behave as passive tracers, whereas particles with $St \to \infty$ will be insensitive to the flow field.

In the rest of this paper, it turns out to be practical to rewrite the equations of motions in a rotating reference frame:

$$\frac{d\boldsymbol{\xi}_p}{dt} = \boldsymbol{v}_p, \tag{20}$$

$$\frac{d\boldsymbol{v}_p}{dt} = \frac{1}{St}(\boldsymbol{v}_g - \boldsymbol{v}_p) + 2\dot{\theta}_v \wedge \boldsymbol{v}_p + \dot{\theta}_v^2 \boldsymbol{\xi}_p, \tag{21}$$

where $\boldsymbol{\xi}$ and $\boldsymbol{v}$ denote the position and the velocity in the rotating frame. The two additional terms on the RHS, which depend on the rotation rate $\dot{\theta}_v$, are the Coriolis force and the centrifugal force.

Consider the trajectories of two particles, which are initially very close. The initial differences in position and velocity are small and therefore denoted by $\delta\boldsymbol{\xi}_p$ and $\delta\boldsymbol{v}_p$, respectively. Now, the 4-dimensional separation vector $\boldsymbol{R} \equiv [\delta\boldsymbol{\xi}_p, \delta\boldsymbol{v}_p]^T$ is introduced (see also [2]). If the separation between the two trajectories is small, the time development of the separation vector can be expressed in the following form:

$$\frac{d}{dt}\boldsymbol{R}(t) = \boldsymbol{M}\boldsymbol{R}(t), \tag{22}$$

where the matrix $\boldsymbol{M}$ reads:

$$\boldsymbol{M} = \begin{pmatrix} 0 & 0 & 1 & 0 \\ 0 & 0 & 0 & 1 \\ \frac{1}{St}\frac{\partial v_g}{\partial \xi} + \dot{\theta}_v^2 & \frac{1}{St}\frac{\partial v_g}{\partial \eta} & -\frac{1}{St} & 2\dot{\theta}_v \\ \frac{1}{St}\frac{\partial v_g}{\partial \xi} & \frac{1}{St}\frac{\partial v_g}{\partial \eta} + \dot{\theta}_v^2 & -2\dot{\theta}_v & \frac{1}{St} \end{pmatrix}. \tag{23}$$

Clearly, the separation vector can only be used in smooth flows for which the gradient of the velocity field exists. This will be no problem in our test cases. When all eigenvalues of the matrix $\boldsymbol{M}$ have a real part smaller than zero, the separation vector goes to 0 for $t \to \infty$. This means that the two particles converge towards each other.

3 Results: heavy particle motion in a bounded one-vortex flow

Now we investigate the motion of heavy particles in bounded vortex flows. Each particle is traced individually by using a fourth-order Runge–Kutta method. First, the equations of motion (Equation 18) are integrated using a fixed time step. Subsequently, the same integration is done with half of the time step. This procedure is repeated until the difference between two subsequent solutions is below a certain preset level.

In Figure 3, two different particle trajectories are plotted for the case $r_v = 0.5$. One particle, released on $(\xi, \eta) = (0.25, -0.2)$, is quickly expelled from the circular boundary and moves increasingly far away from the origin. The other particle, released on $(\xi, \eta) = (0, 0)$, is trapped in one particular attraction point within the circular domain.

This behavior is better perceptible when the positions of a group of heavy particles in the course of time are considered. In this case, we have taken 7495 particles which are uniformly distributed over the circular domain at the start of the simulation ($t = 0$). The particle positions are plotted in the frame rotating with the vortex in Figure 4. Clearly, many particles accumulate in the same point. This means that in physical space the particles approach to a circular trajectory periodic with the vortex motion.

The particle accumulation within the circular boundary occurs for a wide variety of initial conditions for the particle position. As an illustration, the particle trapping efficiency P, defined as:

$$P \equiv \frac{(\text{number of particles with } r < 1 \text{ for } t \to \infty)}{(\text{total number of initially uniformly distributed particles})} \times 100\%, \tag{24}$$

is calculated for three different configurations of a bounded one-vortex flow: r_v is taken 0.3, 0.5 and 0.7, respectively. The results are plotted in Figure 5.

For the particle accumulation to occur, two conditions must be met: firstly, a fixed point of the dynamical equations (20) and (21) can be found, and secondly, the fixed point has to be stable, thus attracting particles. Both conditions will be treated in the remainder of this section.

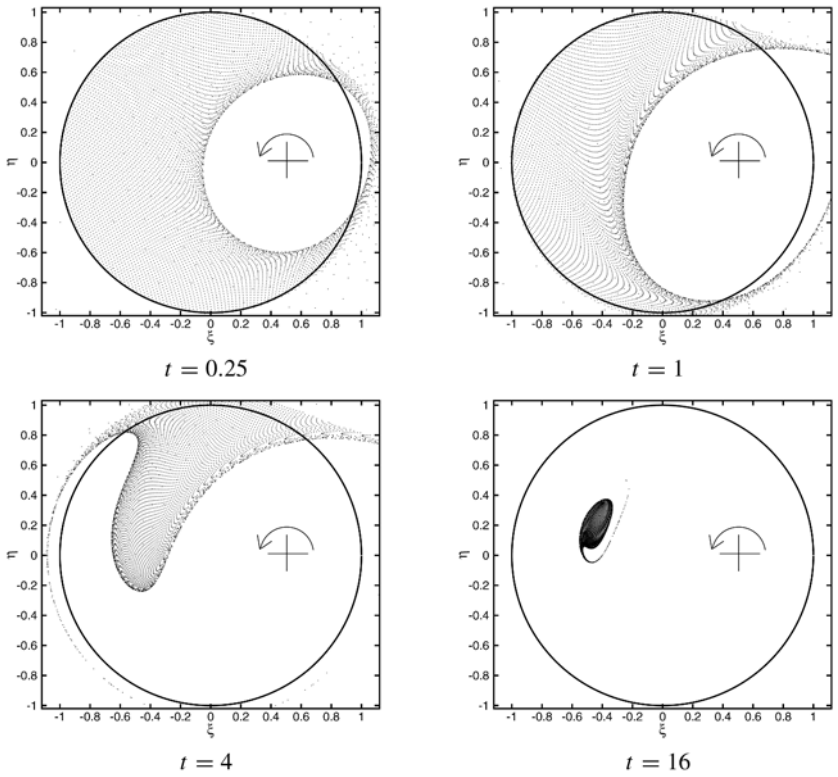

Fig. 4. Distribution of heavy particles in one-vortex system; $St = 0.6$.

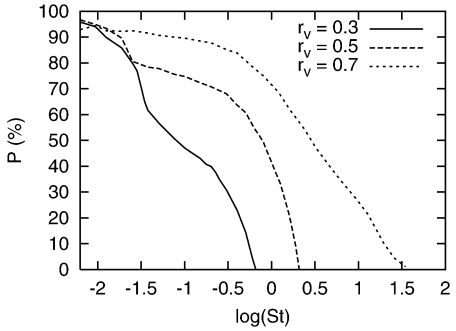

Fig. 5. Percentage of particle trapping as a function of St, for three different vortex configurations.

3.1 Location of fixed points in co-rotating frame

A trapped particle, rotating with the same speed as the vortex, has zero velocity in the co-rotating frame. Hence, the RHS of Equations (20) and (21) goes to 0 for such

a particle in the fixed point, say $\boldsymbol{\xi}^*$. In order for this to happen, the Stokes drag has to balance the centrifugal acceleration:

$$(\boldsymbol{v}_g(\boldsymbol{\xi}^*)) + St\dot{\theta}_v^2\boldsymbol{\xi}^* = 0. \tag{25}$$

From this equation, it follows immediately that for small Stokes numbers also $\boldsymbol{v}_g$ has to be small. Consequently, in the limit of $St \downarrow 0$ the fixed point is situated near a stagnation point of the gas velocity in the co-rotating frame. The only reasonable candidate for this is the elliptic stagnation point situated on the negative ξ-axis, since the hyperbolic stagnation points are unstable by definition.

3.2 Stability of fixed points in co-rotating frame

Now a linear stability analysis is made of the particle approaching the fixed point $\boldsymbol{\xi}^*$. If the particle is close enough to the attraction point, its equation of motion can be approximated by:

$$\frac{d}{dt}\boldsymbol{R}^* = \boldsymbol{M}\boldsymbol{R}^*, \tag{26}$$

where $\boldsymbol{R}^*$ is a vector denoting the separation between the attracted particle and the fixed point:

$$\boldsymbol{R}^* \equiv [\boldsymbol{\xi}_p - \boldsymbol{\xi}^*, \boldsymbol{v}_p]^T. \tag{27}$$

The matrix $\boldsymbol{M}$ is given in Equation (23). In this case, the matrix can be evaluated in the fixed point.

If the real parts of all eigenvalues $\lambda_1, \ldots, \lambda_4$ of $\boldsymbol{M}$ are negative, the fixed point $\boldsymbol{\xi}^*$ is called stable. The eigenvalues read:

$$\lambda_{1,2,3,4} = \frac{-1 \pm \sqrt{1 - 4\dot{\theta}_v^2 St^2 \pm 4St\sqrt{-\mathcal{H}^*}}}{2St}, \tag{28}$$

where $\mathcal{H}^*$ denotes the Hessian, defined in Equation (14), evaluated in the fixed point. For small Stokes numbers, the fixed point is situated close to the elliptic stagnation point, so that $\mathcal{H}^* > 0$. Then, the eigenvalues can be approximated by:

$$\lambda_{1,2,3,4} \simeq \frac{-1 \pm 1}{2St} + St\left(\mathcal{H}^* - \dot{\theta}_v^2\right) \pm i\sqrt{\mathcal{H}^*}. \tag{29}$$

Using the property of the total Hessian in a steadily rotating reference frame, given in Equation (16), we obtain:

$$\lambda_{1,2,3,4} \simeq \frac{-1 \pm 1}{2St} - St\left\{\overline{\Psi}_{\xi\xi}^2 + \overline{\Psi}_{\xi\eta}^2\right\} \pm i\sqrt{\mathcal{H}^*}. \tag{30}$$

Hence, for small Stokes numbers, the real part is always smaller than 0, indicating that the fixed point is stable and does attract particles. So, if a counter-rotating elliptic stagnation point exists in some steadily rotating reference frame, small heavy particles are attracted to it.

When the Stokes number becomes larger, the fixed point will be situated further away from the center of the elliptic island. Then, particles have too much inertia and will be expelled from the domain. Hence, the number of particles trapped inside the domain decreases with increasing Stokes number. This behavior is visible in Figure 5.

Please note that the stability analysis above is not only restricted to the flow induced by a point vortex in a circular domain, but can as well be applied to an other incompressible inviscid flow, as long as it is steady in some steadily rotating reference frame. Examples of this comprise the motion of vortices on a regular polygon on an infinite plane or on a disk (whose origin coincides with the barycenter) or an approximation of the flow field on a Keplerian disk as given by Chavanis [3]. Chavanis prescribes an anticyclonic vortex region a priori; in our case, the elliptic island is formed naturally just by the presence of a cyclonic vortex. Still, the results found here are qualitatively in correspondence with those obtained by Chavanis: small heavy particles are attracted towards a fixed point in a steady anticyclonic island.

4 Conclusions

In this paper, the trajectories of heavy particles in a bounded point vortex flow have been calculated numerically. The simulations are based on a one-way coupling. The results reveal that heavy particles may accumulate in certain regions where the centrifugal and the drag forces acting on the particles balance each other, thus causing an equilibrium trajectory.

A linear stability analysis shows that particles are always attracted to a fixed point, as long as the Stokes number is below a critical value, depending on the particular flow properties. The analysis is shown to be valid not only for point vortex flows but also for any steadily rotating flow field which can be expressed in terms of a stream function.

These results can also be relevant for the swirling pipe flow discussed in Section 1. Small inertial particles tend to accumulate in regions far away from the helical vortex filament, but inside the pipe. Although many other effects play a role in the particle motion on small scales, the inertia is believed to be a dominant effect in macro-scale motion of particles in this situation.

References

1. Alekseenko, S.V., Kuibin, P.A., Okulov, V.L. and Shtork, S.I., 1999, *J. Fluid Mech.* **382**, 195–243.
2. Bec, J., 2003, *Phys. Fluids* **15**(11), L81–L84.
3. Chavanis, P.H., 2000, *Astron. Astrophys.* **356**, 1089–1111.
4. Crowe, C.T., Gore, R. and Troutt, T.R., 1985, *Particulate Science and Technology*, **3**, 149–158.

5. Druzhinin, O.A., 1995, *Phys. Fluids* **7**(9), 2132–2142.
6. Marcu, B., Meiburg, E. and Newton, P.K., 1995, *Phys. Fluids* **7**(2), 400–410.
7. Maxey, M.R., 1990, *Phil. Trans. R. Soc. London A* **333**, 289–307.
8. Maxey, M.R. and Riley, J.J., 1983, *Phys. Fluids* **26**(4), 883–889.
9. Newton, P.K., 2001, *The N-Vortex Problem – Analytical Techniques*, Springer Verlag, Berlin.
10. Provenzale, A., 1999, *Ann. Rev. Fluid Mech.* **31**, 55–93.
11. Squires, K.D. and Eaton, J.K., 1991, *Phys. Fluids* **3**(5), 1169–1178.